Mathematics

https://www.aimspress.com/journal/Math

AIMS Mathematics, 9(11): 30153–30173.
DOI: 10.3934/math.20241456
Received: 30 August 2024
Revised: 17 October 2024
Accepted: 18 October 2024
Published: 23 October 2024

*Research article*

# Kink soliton solution of integrable Kairat-X equation via two integration algorithms

**Raed Qahiti[1], Naher Mohammed A. Alsafri[2,*], Hamad Zogan[3] and Abdullah A. Faqihi[4]**

[1] Department of Mathematics, Faculty of Science, Jazan University, P.O. Box 2097, Jazan 45142, kingdom of Saudi Arabia

[2] Department of Mathematics, Faculty of Science, University of Jeddah, kingdom of Saudi Arabia

[3] Department of Computer Science, College of Computer Science and Information Technology, Jazan University, Jazan 45142, kingdom of Saudi Arabia

[4] Department of Industrial Engineering, College of Engineering and Computer Science, Jazan University, P.O. Box 706, Jazan 45142, kingdom of Saudi Arabia

* **Correspondence:** Email: nmalsafri@uj.edu.sa.

**Abstract:** In order to establish and assess the dynamics of kink solitons in the integrable Kairat-X equation, which explains the differential geometry of curves and equivalence aspects, the present investigation put forward two variants of a unique transformation-based analytical technique. These modifications were referred to as the generalized $(r + \frac{G'}{G})$-expansion method and the simple $(\frac{G'}{G})$-expansion approach. The proposed methods spilled over the aimed Kairat-X equation into a nonlinear ordinary differential equation by means of a variable transformation. Immediately following that, it was presumed that the resultant nonlinear ordinary differential equation had a closed form solution, which turned it into a system of algebraic equations. The resultant set of algebraic equations was solved to find new families of soliton solutions which took the forms of hyperbolic, rational and periodic functions. An assortment of contour, 2D and 3D graphs were used to visually show the dynamics of certain generated soliton solutions. This indicated that these soliton solutions likely took the structures of kink solitons prominently. Moreover, our proposed methods demonstrated their use by constructing a multiplicity of soliton solutions, offering significant understanding into the evolution of the focused model, and suggesting possible applications in dealing with related nonlinear phenomena.

**Keywords:** nonlinear partial differential equations; $(\frac{G'}{G})$-expansion methods; integrable model; closed-form solutions; soliton phenomena
**Mathematics Subject Classification:** 34A25, 35C08, 35D99

## 1. Introduction

Nonlinear partial differential equations (NPDEs) are a vital arsenal in numerous scientific disciplines because they provide a stable basis for modeling complex phenomena that defy linear approximations [1–3]. They are commonly employed in physics to explain turbulent motion, dynamics of fluids, and propagation of waves. They also provide insight on a wide range of problems, involving as irregularities in the weather and particle behavior. Such structures are used by engineers for evaluating electrical thermal transfer, circuits, and mechanics of structures in order to develop efficient mechanisms. In the biological sciences, NPDEs can be employed to model a variety of processes, including infection dissemination, demographic change, and neural network function. They are used by scientists studying the environment to comprehend ecological changes in many contexts, like the climate projections and functioning of ecosystems. Consequently, in many scientific domains, NPDEs are essential tools for tackling complicated real-world issues and are vital to modern scientific research [4–6].

Researchers often move toward analytical solutions when tackling NPDEs to overcome the inherent shortcomings of numerical approaches, such as the demand for complex computer specifications, mistakes, and large amounts of processing power. Analytical solutions are succinct mathematical claims that, with little computational effort, offer profound understanding of the underlying behavior of the system. Recently, explicit solutions–especially those that resemble soliton–have garnered a lot of attention as nonlinear science has elevated them to a separate field of study [7–9]. Because of these unique features, soliton theory has gained more prominence. After interaction and stability, the soliton maintains its shape and velocity. Rogue, cuspon, cnoidal, peregrine, anti-kink dromion, dark, lump, bright, dark-bright, loop, periodic, grey, hump, kink, compacton and black soliton are only a few of the various varieties of soliton. For a considerable while now, physicists and applied mathematics have been fascinated by soliton applications in NPDEs. Several analytical methods have been put forth to assess and characterize the soliton behavior in NPDEs, which include the Kudryashov approach [10], $(\frac{G'}{G})$-expansion approach [11], Sardar sub-equation technique [12], exp-function method [13], sub-equation technique [14], tan-cot function approach [15], extended direct algebraic methods [16], Khater method [17] and many others [18–20]. However, this research drives the employee $(\frac{G'}{G})$-expansion method which was first introduced by Wang et al. [21] and is a special sub-case of modified extended tanh expansion method [22].

The primary goals of this work are to produce and assess the dynamics of kink soliton in the Kairat-X equation (K-XE). The recommended generalized $(r + \frac{G'}{G})$-expansion method and simple $(\frac{G'}{G})$-expansion method to convert K-XE to nonlinear ordinary differential equations (NODE) both employ a wave transformation. Under the assumption of a series form solution, NODE is further turned into an algebraic system of equations. By solving this set of equations, many new soliton solutions for K-XE in the form of hyperbolic, rational and periodic functions are obtained, indicating the efficacy of the proposed methods. This integrable model explains the differential geometry of curves and equivalence aspects. K-XE is described as [23, 24]:

$$s_{tt} - 3\left(s_t s_x\right)_x + s_{xxxt} = 0, \tag{1}$$

whereby $s = s(x, t)$. This model has numerous applications in applied sciences such as geophysics, optical fiber, mathematical physics, laser optics, nonlinear dynamics, nonlinear optics, engineering and communication systems.

There is a dearth of research in the literature on Kairat equations with respect to fractional and integer form. For instance, Roy et al. [25] contains solutions to the K-XE for lump-kink waves, multi-shocks, and kink-breather. Ghazanfar et al. [26] has identified soliton, rational, and elliptic solutions to the Kairat-II equation using the Hirota bilinear form. Awadalla et al. used soliton solutions, the advanced Kudryashov method, and the modified simple equation approach in [24] to solve two Kairat equations, namely the K-XE and Kairat-II equations, in the context of $M$-fractional derivatives. The optical soliton solutions for the Kairat-II problem were developed by Tipu et al. using extended direct algebraic method (EDAM) [27]. Iqbal et al. eventually employed an enhanced variation of the simple equation approach to investigate many exact soliton solutions such as kink wave solitons, bright-dark solutions, dark and peakon bright solitons, bright solitons, anti-kink wave solutions, solitary wave structure and dark solitons for fractional K-XE with a different ansatz. They have retrieved soliton solutions to the nonlinear fractional K-XE efficiently [28]. These solutions offer a stimulating physical framework for dark solitons, traveling waves, kink solitons, peakon solitons, mixed solitons, anti-kink solitons, bright solitons and solitary waves. Nevertheless, the goal of this work is to show how well the two suggested variations of the $(\frac{G'}{G})$-expansion method work to assess the dynamics of kink solitons in K-XE, as stated in Eq (1).

The remaining parts of the study are arranged in the following order: In Section 2, we go over how the recommended approaches function. We utilize these methods to build soliton solutions for the K-XE in Section 3. In Section 4, we present the visual illustrations of several kink soliton solutions. Meanwhile, Section 5 concludes our study.

## 2. The operational mechanism of $(\frac{G'}{G})$-expansion methods

In this section of our investigation, the procedures of the $(\frac{G'}{G})$-expansion methods are described, concentrating on solving the following type of general NPDE [11]:

$$R(s, s_t, s_{v_1}, s_{v_2}, ss_{v_1}, \dots) = 0, \tag{2}$$

where $s = s(t, v_1, v_2, v_3, \dots, v_j)$.

Equation (2) is resolved employing the subsequent technique:

1) After transforming the framework $s(t, v_1, v_2, v_3, \dots, v_j) = S(\vartheta)$, where $\vartheta$ is the wave variable such that $\vartheta = \vartheta(t, v_1, v_2, v_3, \dots, v_j)$, when this transformation is applied to Eq (2), we get the subsequent NODE:

$$J(S, S'S, S', \dots) = 0, \tag{3}$$

where $S' = \frac{dS}{d\vartheta}$. Rarely, the integration of Eq (3) may make the NODE susceptible to the homogeneous balancing principle.

2) Next, using the modified $(\frac{G'}{G})$-expansion approach, we presume any of the subsequent series form solutions for Eq (3):

**a)** Using the simple $(\frac{G'}{G})$-expansion method, we choose the following series form solution [11]:

$$S(\vartheta) = \sum_{j=-M}^{M} \tau_j (\frac{G'(\vartheta)}{G(\vartheta)})^j, \tag{4}$$

**b)** Using the $(r+\frac{G'}{G})$-expansion approach, we choose the ensuing series form solution [11]:

$$S(\vartheta)=\sum_{j=-M}^{M}\tau_j(r+\frac{G'(\vartheta)}{G(\vartheta)})^j;\quad r\ \in\ R, \tag{5}$$

where $\tau_j(-M\leq j\leq M)$ are coefficients with restriction and $\tau_M^2+\tau_{-M}^2\neq 0$, must be calculated later. Equations (4) and (5) yield the balance number $M$, a positive integer, which may be found using the homogeneous balance from the nonlinear components and the derivative that corresponds with the highest order terms in Eq (3). Use the following mathematical formulas to get the balance number $M$ more precisely [29]:

$$D(\frac{d^{\eta}S}{d\vartheta^{\eta}})=M+\eta,\ \text{ and }\ D(S^{\zeta}(\frac{d^{\eta}S}{d\vartheta^{\eta}})^{n})=M\zeta+n(\eta+M), \tag{6}$$

where $D$ expresses degree of $S(\vartheta)$ and $\eta,\zeta$, and $n$ are positive integers.

Moreover, Eqs (4) and (5)'s function $G(\vartheta)$ solves the following second-order linear ODE:

$$G''(\vartheta)+\nu G'(\vartheta)+\omega G(\vartheta)=0, \tag{7}$$

where $\nu,\omega$ are real constants.

Furthermore, using the generic solution of Eq (7), we obtain:

$$\left(\frac{G'(\vartheta)}{G(\vartheta)}\right)=\begin{cases}\frac{1}{2}\frac{\sqrt{Z}\left(\varepsilon_1\sinh\left(\frac{1}{2}\sqrt{Z}\vartheta\right)+\varepsilon_2\cosh\left(\frac{1}{2}\sqrt{Z}\vartheta\right)\right)}{\varepsilon_1\cosh\left(\frac{1}{2}\sqrt{Z}\vartheta\right)+\varepsilon_2\sinh\left(\frac{1}{2}\sqrt{Z}\vartheta\right)}-\frac{1}{2}\nu, & Z>0,\\ \frac{1}{2}\frac{\sqrt{-Z}\left(-\varepsilon_1\sin\left(\frac{1}{2}\sqrt{-Z}\vartheta\right)+\varepsilon_2\cos\left(\frac{1}{2}\sqrt{-Z}\vartheta\right)\right)}{\varepsilon_1\cos\left(\frac{1}{2}\sqrt{-Z}\vartheta\right)+\varepsilon_2\sin\left(\frac{1}{2}\sqrt{-Z}\vartheta\right)}-\frac{1}{2}\nu, & Z<0,\\ \frac{\varepsilon_2}{\varepsilon_1+\varepsilon_2\vartheta}-\frac{1}{2}\nu, & Z=0,\end{cases} \tag{8}$$

where $Z=\nu^2-4\omega$ and $\varepsilon_1$ and $\varepsilon_2$ in Eq (8) are arbitrary constants.

3) Next, we insert Eqs (4) and (5) into Eq (3) and collect all terms that have the same power of $(\frac{G'(\vartheta)}{G(\vartheta)})$.

4) With all of the coefficients of the generated polynomial $(\frac{G'(\vartheta)}{G(\vartheta)})^j$ corresponding to zero, a set of nonlinear algebraic equations in $\tau_j(j=-M...,M)$, $\nu$, $\omega$, and other required parameters are obtained.

5) The system that emerges is solved with the Maple tool to determine the unknown parameters.

6) The values expected from step 5 are then substituted into Eqs (4) and (5) to build families of soliton solutions for Eq (2).

## 3. The implementation of $(\frac{G'}{G})$-expansion methods to K-XE

In this part, we expand our $(\frac{G'}{G})$-expansion methods to establish fresh soliton solutions for Eq (1). We start with the wave transformation given below:

$$s(x,t)=S(\vartheta)\quad\text{with}\quad\vartheta=kx+\phi t+\gamma. \tag{9}$$

The given transformation converts Eq (1) into the subsequent integer order NODE:

$$\phi S''(\vartheta)-3k^2((S'(\vartheta))^2)'+k^3S^{(iv)}(\vartheta)=0. \tag{10}$$

Using Eq (10) and one-time integration with respect to $\vartheta$ produces:

$$\phi S'(\vartheta) - 3k^2(S'(\vartheta))^2 + k^3 S'''(\vartheta) + \kappa = 0, \tag{11}$$

where $\kappa$ symbolizes the integration constant. In Eq (11) by using the homogeneous balance [29] between the terms $-3k^2(S'(\vartheta))^2$ and $k^3S'''(\vartheta)$, suggests that $2M + 2 = 3 + M$ and yields $M = 1$.

### 3.1. The execution of $(\frac{G'}{G})$-expansion method

To start, we want to solve K-XE using the simple $(\frac{G'}{G})$-expansion method. Substituting $M = 1$ in Eq (4) yields the following closed series form solution for Eq (11):

$$S(\vartheta) = \sum_{j=-1}^{1} \tau_j \left(\frac{G'(\vartheta)}{G(\vartheta)}\right)^j. \tag{12}$$

By putting Eq (12) in Eq (11) and combining all terms with the same exponents of $G(\vartheta)$, an equation in $G(\vartheta)$ is obtained. By setting the coefficients to zero, the resultant statement can be simplified to the underlying nonlinear system of nine algebraic equations:

$$-k^2\tau_{-1}{}^2\omega^2 + 2k^3\tau_{-1}\omega^3 = 0,$$

$$2k^3\tau_{-1}\nu\omega^2 - k^2\tau_{-1}{}^2\nu\omega = 0,$$

$$6k^2\tau_{-1}\omega^2\tau_1 + 8k^3\tau_{-1}\omega^2 + \phi\tau_{-1}\omega + 7k^3\tau_{-1}\nu^2\omega - 3k^2\tau_{-1}{}^2\nu^2 - 6k^2\tau_{-1}{}^2\omega = 0,$$

$$12k^2\tau_{-1}\nu\tau_1\omega + \phi\tau_{-1}\nu + k^3\tau_{-1}\nu^3 - 6k^2\tau_{-1}{}^2\nu + 8k^3\tau_{-1}\nu\omega = 0,$$

$$\begin{aligned}&-3k^2\tau_1{}^2\omega^2 - k^3\tau_1\nu^2\omega + 6k^2\tau_{-1}\nu^2\tau_1 - \phi\tau_1\omega + 2k^3\tau_{-1}\omega\\ &+\kappa + k^3\tau_{-1}\nu^2 - 2k^3\tau_1\omega^2 + \phi\tau_{-1} + 12k^2\tau_{-1}\omega\tau_1 - 3k^2\tau_{-1}{}^2 = 0,\end{aligned}$$

$$-k^3\tau_1\nu^3 - \phi\tau_1\nu + 12k^2\tau_{-1}\nu\tau_1 - 8k^3\tau_1\nu\omega - 6k^2\tau_1{}^2\nu\omega = 0,$$

$$-8k^3\tau_1\omega - 7k^3\tau_1\nu^2 + 6k^2\tau_{-1}\tau_1 - 3k^2\tau_1{}^2\nu^2 - \phi\tau_1 - 6k^2\tau_1{}^2\omega = 0,$$

$$2k^3\tau_1\nu + k^2\tau_1{}^2\nu = 0,$$

$$2k^3\tau_1 + k^2\tau_1{}^2 = 0.$$

When Maple handles the created system, the following sets of solutions appear:

**Case 1.1.**

$$\tau_1 = 0, \tau_0 = \tau_0, \tau_{-1} = 2k\omega, k = k, \kappa = 0, \phi = -k^3 Z. \tag{13}$$

**Case 1.2.**

$$\tau_1 = -2k, \tau_0 = \tau_0, \tau_{-1} = 0, k = k, \kappa = 0, \phi = -k^3 Z. \tag{14}$$

Taking into consideration Case 1.1, and using Eqs (9) and (12) with the associated general solution in Eq (8), we form the given families of soliton solutions for K-XE stated in Eq (1):

**Family 1.1.1.** In the course of $Z > 0$,

(i) In the course of $\varepsilon_1 \neq 0$, $\varepsilon_2 \neq 0$,

$$s_{1,1,1}(x,t) = 2\,k\omega\left(\frac{1}{2}\,\frac{\sqrt{Z}\left(\varepsilon_1 \sinh\left(\frac{1}{2}\,\sqrt{Z}(kx - k^3Zt + \gamma)\right) + \varepsilon_2 \cosh\left(\frac{1}{2}\,\sqrt{Z}(kx - k^3Zt + \gamma)\right)\right)}{\varepsilon_1 \cosh\left(\frac{1}{2}\,\sqrt{Z}(kx - k^3Zt + \gamma)\right) + \varepsilon_2 \sinh\left(\frac{1}{2}\,\sqrt{Z}(kx - k^3Zt + \gamma)\right)} - \frac{1}{2}\,\nu\right)^{-1} + \tau_0. \tag{15}$$

(ii) In the course of $\varepsilon_1 = 0$, $\varepsilon_2 \neq 0$,

$$s_{1,1,2}(x,t) = 2\,\frac{k\omega}{\frac{1}{2}\,\sqrt{Z}\coth\left(\frac{1}{2}\,\sqrt{Z}(kx - k^3Zt + \gamma)\right) - \frac{1}{2}\,\nu} + \tau_0. \tag{16}$$

(iii) In the course of $\varepsilon_1 \neq 0$, $\varepsilon_2 = 0$,

$$s_{1,1,3}(x,t) = 2\,\frac{k\omega}{\frac{1}{2}\,\sqrt{Z}\tanh\left(\frac{1}{2}\,\sqrt{Z}(kx - k^3Zt + \gamma)\right) - \frac{1}{2}\,\nu} + \tau_0. \tag{17}$$

**Family 1.1.2.** In the course of $Z < 0$,

(i) In the course of $\varepsilon_1 \neq 0$, $\varepsilon_2 \neq 0$,

$$s_{1,1,4}(x,t) = 2\,k\omega\left(\frac{1}{2}\,\frac{\sqrt{-Z}\left(-\varepsilon_1 \sin\left(\frac{1}{2}\,\sqrt{-Z}(kx - k^3Zt + \gamma)\right) + \varepsilon_2 \cos\left(\frac{1}{2}\,\sqrt{-Z}(kx - k^3Zt + \gamma)\right)\right)}{\varepsilon_1 \cos\left(\frac{1}{2}\,\sqrt{-Z}(kx - k^3Zt + \gamma)\right) + \varepsilon_2 \sin\left(\frac{1}{2}\,\sqrt{-Z}(kx - k^3Zt + \gamma)\right)} - \frac{1}{2}\,\nu\right)^{-1} + \tau_0. \tag{18}$$

(ii) In the course of $\varepsilon_1 = 0$, $\varepsilon_2 \neq 0$,

$$s_{1,1,5}(x,t) = 2\,\frac{k\omega}{\frac{1}{2}\,\sqrt{-Z}\cot\left(\frac{1}{2}\,\sqrt{-Z}(kx - k^3Zt + \gamma)\right) - \frac{1}{2}\,\nu} + \tau_0. \tag{19}$$

(iii) In the course of $\varepsilon_1 \neq 0$, $\varepsilon_2 = 0$,

$$s_{1,1,6}(x,t) = 2\,\frac{k\omega}{-\frac{1}{2}\,\sqrt{-Z}\tan\left(\frac{1}{2}\,\sqrt{-Z}(kx - k^3Zt + \gamma)\right) - \frac{1}{2}\,\nu} + \tau_0. \tag{20}$$

**Family 1.1.3.** In the course of $Z = 0$,

(i) In the course of $\varepsilon_1 \neq 0$, $\varepsilon_2 \neq 0$,

$$s_{1,1,7}(x,t) = 2\,\frac{k\omega\left(\varepsilon_1 + \varepsilon_2(kx - k^3Zt + \gamma)\right)}{\varepsilon_2} + \tau_0. \tag{21}$$

(ii) In the course of $\varepsilon_1 = 0$, $\varepsilon_2 \neq 0$,

$$s_{1,1,8}(x,t) = 2\,\frac{k\omega}{(kx - k^3Zt + \gamma)^{-1} - \frac{1}{2}\,\nu} + \tau_0. \tag{22}$$

Assuming Case 1.2, and using Eqs (9) and (12) with the associated general solution in Eq (8), we form the given below families of soliton solutions for K-XE stated in Eq (1):

**Family 1.2.1.** In the course of $Z > 0$,

(i) In the course of $\varepsilon_1 \neq 0, \varepsilon_2 \neq 0$,

$$s_{1,2,1}(x,t) = \tau_0 - 2\,k\left(\frac{1}{2}\,\frac{\sqrt{Z}\left(\varepsilon_1 \sinh\left(\frac{1}{2}\,\sqrt{Z}(kx-k^3Zt+\gamma)\right)+\varepsilon_2\cosh\left(\frac{1}{2}\,\sqrt{Z}(kx-k^3Zt+\gamma)\right)\right)}{\varepsilon_1\cosh\left(\frac{1}{2}\,\sqrt{Z}(kx-k^3Zt+\gamma)\right)+\varepsilon_2\sinh\left(\frac{1}{2}\,\sqrt{Z}(kx-k^3Zt+\gamma)\right)}-\frac{1}{2}\,\nu\right). \tag{23}$$

(ii) In the course of $\varepsilon_1 = 0, \varepsilon_2 \neq 0$,

$$s_{1,2,2}(x,t) = \tau_0 - 2\,k\left(\frac{1}{2}\,\sqrt{Z}\coth\left(\frac{1}{2}\,\sqrt{Z}(kx-k^3Zt+\gamma)\right)-\frac{1}{2}\,\nu\right). \tag{24}$$

(iii) In the course of $\varepsilon_1 \neq 0, \varepsilon_2 = 0$,

$$s_{1,2,3}(x,t) = \tau_0 - 2\,k\left(\frac{1}{2}\,\sqrt{Z}\tanh\left(\frac{1}{2}\,\sqrt{Z}(kx-k^3Zt+\gamma)\right)-\frac{1}{2}\,\nu\right). \tag{25}$$

**Family 1.2.2.** In the course of $Z < 0$,

(i) In the course of $\varepsilon_1 \neq 0, \varepsilon_2 \neq 0$,

$$\begin{aligned} &s_{1,2,4}(x,t)\\ =&\tau_0 - 2\,k\left(\frac{1}{2}\,\frac{\sqrt{-Z}\left(-\varepsilon_1 \sin\left(\frac{1}{2}\,\sqrt{-Z}(kx-k^3Zt+\gamma)\right)+\varepsilon_2\cos\left(\frac{1}{2}\,\sqrt{-Z}(kx-k^3Zt+\gamma)\right)\right)}{\varepsilon_1\cos\left(\frac{1}{2}\,\sqrt{-Z}(kx-k^3Zt+\gamma)\right)+\varepsilon_2\sin\left(\frac{1}{2}\,\sqrt{-Z}(kx-k^3Zt+\gamma)\right)}-\frac{1}{2}\,\nu\right). \end{aligned} \tag{26}$$

(ii) In the course of $\varepsilon_1 = 0, \varepsilon_2 \neq 0$,

$$s_{1,2,5}(x,t) = \tau_0 - 2\,k\left(\frac{1}{2}\,\sqrt{-Z}\cot\left(\frac{1}{2}\,\sqrt{-Z}(kx-k^3Zt+\gamma)\right)-\frac{1}{2}\,\nu\right). \tag{27}$$

(iii) In the course of $\varepsilon_1 \neq 0, \varepsilon_2 = 0$,

$$s_{1,2,6}(x,t) = \tau_0 - 2\,k\left(-\frac{1}{2}\,\sqrt{-Z}\tan\left(\frac{1}{2}\,\sqrt{-Z}(kx-k^3Zt+\gamma)\right)-\frac{1}{2}\,\nu\right). \tag{28}$$

**Family 1.2.3.** In the course of $Z = 0$,

(i) In the course of $\varepsilon_1 \neq 0, \varepsilon_2 \neq 0$,

$$s_{1,2,7}(x,t) = \tau_0 - 2\,\frac{k\varepsilon_2}{\varepsilon_1+\varepsilon_2(kx-k^3Zt+\gamma)}. \tag{29}$$

(ii) In the course of $\varepsilon_1 = 0, \varepsilon_2 \neq 0$,

$$s_{1,2,8}(x,t) = \tau_0 - 2\,k\left((kx-k^3Zt+\gamma)^{-1}-\frac{1}{2}\,\nu\right). \tag{30}$$

### 3.2. *The execution of* $(r + \frac{G'}{G})$*-expansion method*

For K-XE, we now wish to apply the generalized $(r + \frac{G'}{G})$-expansion method. The following is the closed series form solution for Eq (15) where $M = 1$ is used instead of Eq (5),

$$S(\vartheta) = \sum_{j=-1}^{1} \tau_j \left( r + \frac{G'(\vartheta)}{G(\vartheta)} \right)^j . \tag{31}$$

An equation in $G(\vartheta)$ is generated by placing Eq (31) into Eq (11) and gathering all terms with the same powers of $G(\vartheta)$. The resulting expression may be reduced to the proper system of nine nonlinear algebraic equations by setting the coefficients to zero:

$$\begin{aligned} &-2k^3\tau_{-1}\omega^2r^2 - 6k^2\omega^2\tau_{-1}\tau_1r^2 - k^3\tau_{-1}\nu^2\omega r^2 - \kappa r^4 + \phi\omega\tau_1r^4 + 3k^2\omega^2{\tau_1}^2r^4 \\ &-6k^3\tau_{-1}\omega^3 + k^3\tau_1\nu^2\omega r^4 + 6k^3\tau_{-1}\omega^2\nu r - \phi\omega\tau_{-1}r^2 + 2k^3\tau_1\omega^2r^4 + 3k^2\omega^2{\tau_{-1}}^2 = 0, \end{aligned}$$

$$\begin{aligned} &4\phi\omega\tau_1r^3 - 4\kappa r^3 + 12k^2\omega^2{\tau_1}^2r^3 + 10k^3\tau_{-1}\nu^2\omega r - 12k^3\tau_{-1}\omega^2\nu + 4k^3\tau_1\nu^2\omega r^3 + 6k^2\nu\omega{\tau_1}^2r^4 \\ &-k^3\tau_{-1}\nu^3r^2 + k^3\tau_1\nu^3r^4 - 12k^2\nu\omega\tau_{-1}\tau_1r^2 - 2\phi\omega\tau_{-1}r + 6k^2\nu\omega{\tau_{-1}}^2 - 12k^2\omega^2\tau_{-1}\tau_1r \\ &+8k^3\tau_1\nu\omega r^4 + 8k^3\tau_{-1}\omega^2r + \phi\nu\tau_1r^4 + 8k^3\tau_1\omega^2r^3 - 8k^3\tau_{-1}\nu\omega r^2 - \phi\nu\tau_{-1}r^2 = 0, \end{aligned}$$

$$\begin{aligned} &-6\kappa r^2 - 24k^2\nu\omega\tau_{-1}\tau_1r - \phi\omega\tau_{-1} - \phi\tau_{-1}r^2 + 6k^2\omega{\tau_{-1}}^2 + 3k^2\nu^2{\tau_{-1}}^2 - 8k^3\tau_{-1}\omega^2 \\ &+\phi\tau_1r^4 - 12k^2\omega\tau_{-1}\tau_1r^2 + 20k^3\tau_{-1}\nu\omega r + 32k^3\tau_1\nu\omega r^3 + 6k^3\tau_1\nu^2\omega r^2 + 24k^2\nu\omega{\tau_1}^2r^3 \\ &-6k^2\nu^2\tau_{-1}\tau_1r^2 - 6k^2\omega^2\tau_{-1}\tau_1 - 7k^3\tau_{-1}\nu^2\omega + 4\phi\nu\tau_1r^3 - 2\phi\nu\tau_{-1}r + 18k^2\omega^2{\tau_1}^2r^2 \\ &+6k^2\omega{\tau_1}^2r^4 + 3k^2\nu^2{\tau_1}^2r^4 + 4k^3\tau_{-1}\nu^3r - 7k^3\tau_{-1}\nu^2r^2 - 8k^3\tau_{-1}\omega r^2 \\ &+4k^3\tau_1\nu^3r^3 + 12k^3\tau_1\omega^2r^2 + 7k^3\tau_1\nu^2r^4 + 8k^3\tau_1\omega r^4 + 6\phi\omega\tau_1r^2 = 0, \end{aligned}$$

$$\begin{aligned} &-4\kappa r - 8k^3\tau_{-1}\nu\omega + 12k^2\nu^2{\tau_1}^2r^3 + 12k^2\omega^2{\tau_1}^2r + 24k^2\omega{\tau_1}^2r^3 + 6\phi\nu\tau_1r^2 + 4\phi\omega\tau_1r \\ &+6k^2\nu{\tau_1}^2r^4 + 10k^3\tau_{-1}\nu^2r + 8k^3\tau_{-1}\omega r - 12k^3\tau_{-1}\nu r^2 + 6k^3\tau_1\nu^3r^2 + 8k^3\tau_1\omega^2r + 28k^3\tau_1\nu^2r^3 \\ &+32k^3\tau_1\omega r^3 + 12k^3\tau_1\nu r^4 - 12k^2\nu\omega\tau_{-1}\tau_1 - 12k^2\nu^2\tau_{-1}\tau_1r + 36k^2\nu\omega{\tau_1}^2r^2 - 24k^2\omega\tau_{-1}\tau_1r \\ &+4k^3\tau_1\nu^2\omega r - 12k^2\nu\tau_{-1}\tau_1r^2 + 48k^3\tau_1\nu\omega r^2 - k^3\tau_{-1}\nu^3 + 4\phi\tau_1r^3 + 6k^2\nu{\tau_{-1}}^2 - \phi\nu\tau_{-1} - 2\phi\tau_{-1}r = 0, \end{aligned}$$

$$\begin{aligned} &3k^2{\tau_{-1}}^2 - \phi\tau_{-1} - \kappa - 6k^3\tau_{-1}r^2 + \phi\omega\tau_1 + 3k^2{\tau_1}^2r^4 + 2k^3\tau_1\omega^2 + 3k^2\omega^2{\tau_1}^2 \\ &+6k^3\tau_1r^4 - k^3\tau_{-1}\nu^2 - 2k^3\tau_{-1}\omega + 6\phi\tau_1r^2 + 24k^2\nu\omega{\tau_1}^2r - 24k^2\nu\tau_{-1}\tau_1r + 32k^3\tau_1\nu\omega r \\ &-12k^2\omega\tau_{-1}\tau_1 + 36k^2\omega{\tau_1}^2r^2 - 6k^2\tau_{-1}\tau_1r^2 - 6k^2\nu^2\tau_{-1}\tau_1 + 18k^2\nu^2{\tau_1}^2r^2 + 6k^3\tau_{-1}\nu r \\ &+4k^3\tau_1\nu^3r + k^3\tau_1\nu^2\omega + 42k^3\tau_1\nu^2r^2 + 48k^3\tau_1\omega r^2 + 48k^3\tau_1\nu r^3 + 4\phi\nu\tau_1r + 24k^2\nu{\tau_1}^2r^3 = 0, \end{aligned}$$

$$\begin{aligned} &12k^2\nu^2{\tau_1}^2r + 8k^3\tau_1\nu\omega + 4\phi\tau_1r - 12k^2\tau_{-1}\tau_1r + k^3\tau_1\nu^3 + 28k^3\tau_1\nu^2r + 32k^3\tau_1\omega r + 12k^2{\tau_1}^2r^3 \\ &-12k^2\nu\tau_{-1}\tau_1 + 72k^3\tau_1\nu r^2 + 36k^2\nu{\tau_1}^2r^2 + 6k^2\nu\omega{\tau_1}^2 + 24k^3\tau_1r^3 + \phi\nu\tau_1 + 24k^2\omega{\tau_1}^2r = 0, \end{aligned}$$

$$\begin{aligned} &7k^3\tau_1\nu^2 + 24k^2\nu{\tau_1}^2r + \phi\tau_1 + 3k^2\nu^2{\tau_1}^2 - 6k^2\tau_{-1}\tau_1 + 6k^2\omega{\tau_1}^2 \\ &+36k^3\tau_1r^2 + 48k^3\tau_1\nu r + 8k^3\tau_1\omega + 18k^2{\tau_1}^2r^2 = 0, \end{aligned}$$

$$12k^2{\tau_1}^2r + 6k^2\nu{\tau_1}^2 + 12k^3\tau_1\nu + 24k^3\tau_1r = 0,$$

$$3k^2{\tau_1}^2 + 6k^3\tau_1 = 0.$$

When Maple handles the created system, the following sets of solutions appear:

**Case 2.1.**

$$\tau_1 = 0, \tau_0 = \tau_0, \tau_{-1} = 2\,kr^2 - 2\,k\nu\,r + 2\,k\omega, k = k, \kappa = 0, \phi = -k^3 Z, r = r. \tag{32}$$

**Case 2.2.**

$$\tau_1 = \tau_1, \tau_0 = \tau_0, \tau_{-1} = 0, k = -\frac{1}{2}\,\tau_1, \kappa = 0, \phi = \frac{1}{8}\,Z{\tau_1}^3, r = r. \tag{33}$$

**Case 2.3.**

$$\tau_1 = \tau_1, \tau_0 = \tau_0, \tau_{-1} = \frac{1}{4}\,Z\nu^2\tau_1, k = -\frac{1}{2}\,\tau_1, \kappa = 0, \phi = \frac{1}{2}\,Z{\tau_1}^3, r = \frac{1}{2}\,\nu. \tag{34}$$

Considering Case 2.1, and using Eqs (9) and (31) with the associated general solution in Eq (8), we form the given families of soliton solutions for K-XE stated in Eq (1):

**Family 2.1.1.** In the course of $Z > 0$,

(i) In the course of $\varepsilon_1 \neq 0$, $\varepsilon_2 \neq 0$,

$$s_{2,1,1}(x,t) = \frac{\left(2\,kr^2 - 2\,k\nu\,r + 2\,k\omega\right)}{\left(r + \frac{1}{2}\,\frac{\sqrt{Z}\left(\varepsilon_1 \sinh\left(\frac{1}{2}\,\sqrt{Z}(kx-k^3Zt+\gamma)\right)+\varepsilon_2\cosh\left(\frac{1}{2}\,\sqrt{Z}(kx-k^3Zt+\gamma)\right)\right)}{\varepsilon_1\cosh\left(\frac{1}{2}\,\sqrt{Z}(kx-k^3Zt+\gamma)\right)+\varepsilon_2\sinh\left(\frac{1}{2}\,\sqrt{Z}(kx-k^3Zt+\gamma)\right)} - \frac{1}{2}\,\nu\right)} + \tau_0. \tag{35}$$

(ii) In the course of $\varepsilon_1 = 0$, $\varepsilon_2 \neq 0$,

$$s_{2,1,2}(x,t) = \frac{2\,kr^2 - 2\,k\nu\,r + 2\,k\omega}{r + \frac{1}{2}\,\sqrt{Z}\coth\left(\frac{1}{2}\,\sqrt{Z}(kx - k^3Zt + \gamma)\right) - \frac{1}{2}\,\nu} + \tau_0. \tag{36}$$

(iii) In the course of $\varepsilon_1 \neq 0$, $\varepsilon_2 = 0$,

$$s_{2,1,3}(x,t) = \frac{2\,kr^2 - 2\,k\nu\,r + 2\,k\omega}{r + \frac{1}{2}\,\sqrt{Z}\tanh\left(\frac{1}{2}\,\sqrt{Z}(kx - k^3Zt + \gamma)\right) - \frac{1}{2}\,\nu} + \tau_0. \tag{37}$$

**Family 2.1.2.** In the course of $Z < 0$,

(i) In the course of $\varepsilon_1 \neq 0$, $\varepsilon_2 \neq 0$,

$$s_{2,1,4}(x,t) = \frac{\left(2\,kr^2 - 2\,k\nu\,r + 2\,k\omega\right)}{\left(r + \frac{1}{2}\,\frac{\sqrt{-Z}\left(-\varepsilon_1 \sin\left(\frac{1}{2}\,\sqrt{-Z}(kx-k^3Zt+\gamma)\right)+\varepsilon_2\cos\left(\frac{1}{2}\,\sqrt{-Z}(kx-k^3Zt+\gamma)\right)\right)}{\varepsilon_1\cos\left(\frac{1}{2}\,\sqrt{-Z}(kx-k^3Zt+\gamma)\right)+\varepsilon_2\sin\left(\frac{1}{2}\,\sqrt{-Z}(kx-k^3Zt+\gamma)\right)} - \frac{1}{2}\,\nu\right)} + \tau_0. \tag{38}$$

(ii) In the course of $\varepsilon_1 = 0$, $\varepsilon_2 \neq 0$,

$$s_{2,1,5}(x,t) = \frac{2\,kr^2 - 2\,k\nu\,r + 2\,k\omega}{r + \frac{1}{2}\,\sqrt{-Z}\cot\left(\frac{1}{2}\,\sqrt{-Z}(kx - k^3Zt + \gamma)\right) - \frac{1}{2}\,\nu} + \tau_0. \tag{39}$$

(iii) In the course of $\varepsilon_1 \neq 0$, $\varepsilon_2 = 0$,

$$s_{2,1,6}(x,t) = \frac{2\,kr^2 - 2\,k\nu\,r + 2\,k\omega}{r - \frac{1}{2}\,\sqrt{-Z}\tan\left(\frac{1}{2}\,\sqrt{-Z}(kx - k^3Zt + \gamma)\right) - \frac{1}{2}\,\nu} + \tau_0. \tag{40}$$

**Family 2.1.3.** In the course of $Z = 0$,

(i) In the course of $\varepsilon_1 \neq 0, \varepsilon_2 \neq 0$,

$$s_{2,1,7}(x,t) = \left(2\,kr^2 - 2\,k\nu\,r + 2\,k\omega\right)\left(r + \frac{\varepsilon_2}{\varepsilon_1 + \varepsilon_2(kx - k^3Zt + \gamma)}\right)^{-1} + \tau_0. \tag{41}$$

(ii) In the course of $\varepsilon_1 = 0, \varepsilon_2 \neq 0$,

$$s_{2,1,8}(x,t) = \frac{2\,kr^2 - 2\,k\nu\,r + 2\,k\omega}{r + (kx - k^3Zt + \gamma)^{-1} - \frac{1}{2}\,\nu} + \tau_0. \tag{42}$$

Considering Case 2.2, and using Eqs (9) and (31) with the associated general solution in Eq (8), we acquire the given families of soliton solutions for K-XE stated in Eq (1):

**Family 2.2.1.** In the course of $Z > 0$,

(i) In the course of $\varepsilon_1 \neq 0, \varepsilon_2 \neq 0$,

$$s_{2,2,1}(x,t) = \tau_0 + \tau_1\left(r + \frac{1}{2}\,\frac{\sqrt{Z}\left(\varepsilon_1\sinh\left(\frac{1}{2}\,\sqrt{Z}(-\frac{1}{2}\,\tau_1 x + \frac{1}{8}\,Z{\tau_1}^3 t + \gamma)\right) + \varepsilon_2\cosh\left(\frac{1}{2}\,\sqrt{Z}(-\frac{1}{2}\,\tau_1 x + \frac{1}{8}\,Z{\tau_1}^3 t + \gamma)\right)\right)}{\varepsilon_1\cosh\left(\frac{1}{2}\,\sqrt{Z}(-\frac{1}{2}\,\tau_1 x + \frac{1}{8}\,Z{\tau_1}^3 t + \gamma)\right) + \varepsilon_2\sinh\left(\frac{1}{2}\,\sqrt{Z}(-\frac{1}{2}\,\tau_1 x + \frac{1}{8}\,Z{\tau_1}^3 t + \gamma)\right)} - \frac{1}{2}\,\nu\right). \tag{43}$$

(ii) In the course of $\varepsilon_1 = 0, \varepsilon_2 \neq 0$,

$$s_{2,2,2}(x,t) = \tau_0 + \tau_1\left(r + \frac{1}{2}\,\sqrt{Z}\coth\left(\frac{1}{2}\,\sqrt{Z}(-\frac{1}{2}\,\tau_1 x + \frac{1}{8}\,Z{\tau_1}^3 t + \gamma)\right) - \frac{1}{2}\,\nu\right). \tag{44}$$

(iii) In the course of $\varepsilon_1 \neq 0, \varepsilon_2 = 0$,

$$s_{2,2,3}(x,t) = \tau_0 + \tau_1\left(r + \frac{1}{2}\,\sqrt{Z}\tanh\left(\frac{1}{2}\,\sqrt{Z}(-\frac{1}{2}\,\tau_1 x + \frac{1}{8}\,Z{\tau_1}^3 t + \gamma)\right) - \frac{1}{2}\,\nu\right). \tag{45}$$

**Family 2.2.2.** In the course of $Z < 0$,

(i) In the course of $\varepsilon_1 \neq 0, \varepsilon_2 \neq 0$,

$$s_{2,2,4}(x,t) = \tau_0 + \tau_1\left(r + \frac{1}{2}\,\frac{\sqrt{-Z}\left(-\varepsilon_1\sin\left(\frac{1}{2}\,\sqrt{-Z}(-\frac{1}{2}\,\tau_1 x + \frac{1}{8}\,Z{\tau_1}^3 t + \gamma)\right) + \varepsilon_2\cos\left(\frac{1}{2}\,\sqrt{-Z}(-\frac{1}{2}\,\tau_1 x + \frac{1}{8}\,Z{\tau_1}^3 t + \gamma)\right)\right)}{\varepsilon_1\cos\left(\frac{1}{2}\,\sqrt{-Z}(-\frac{1}{2}\,\tau_1 x + \frac{1}{8}\,Z{\tau_1}^3 t + \gamma)\right) + \varepsilon_2\sin\left(\frac{1}{2}\,\sqrt{-Z}(-\frac{1}{2}\,\tau_1 x + \frac{1}{8}\,Z{\tau_1}^3 t + \gamma)\right)} - \frac{1}{2}\,\nu\right). \tag{46}$$

(ii) In the course of $\varepsilon_1 = 0, \varepsilon_2 \neq 0$,

$$s_{2,2,5}(x,t) = \tau_0 + \tau_1\left(r + \frac{1}{2}\,\sqrt{-Z}\cot\left(\frac{1}{2}\,\sqrt{-Z}(-\frac{1}{2}\,\tau_1 x + \frac{1}{8}\,Z{\tau_1}^3 t + \gamma)\right) - \frac{1}{2}\,\nu\right). \tag{47}$$

(iii) In the course of $\varepsilon_1 \neq 0, \varepsilon_2 = 0$,

$$s_{2,2,6}(x,t) = \tau_0 + \tau_1\left(r - \frac{1}{2}\,\sqrt{-Z}\tan\left(\frac{1}{2}\,\sqrt{-Z}(-\frac{1}{2}\,\tau_1 x + \frac{1}{8}\,Z{\tau_1}^3 t + \gamma)\right) - \frac{1}{2}\,\nu\right). \tag{48}$$

**Family 2.2.3.** In the course of $Z = 0$,

(i) In the course of $\varepsilon_1 \neq 0, \varepsilon_2 \neq 0$,

$$s_{2,2,7}(x,t) = \tau_0 + \tau_1 \left( r + \frac{\varepsilon_2}{\varepsilon_1 + \varepsilon_2(-\frac{1}{2}\tau_1 x + \frac{1}{8} Z{\tau_1}^3 t + \gamma)} \right). \tag{49}$$

(ii) In the course of $\varepsilon_1 = 0, \varepsilon_2 \neq 0$,

$$s_{2,2,8}(x,t) = \tau_0 + \tau_1 \left( r + (-\frac{1}{2}\tau_1 x + \frac{1}{8} Z{\tau_1}^3 t + \gamma)^{-1} - \frac{1}{2}\nu \right). \tag{50}$$

Considering Case 2.3, and using Eqs (9) and (31) with the associated general solution in Eq (8), we acquire the given families of soliton solutions for K-XE stated in Eq (1):

**Family 2.3.1.** In the course of $Z > 0$,

(i) In the course of $\varepsilon_1 \neq 0, \varepsilon_2 \neq 0$,

$$\begin{aligned} &s_{2,3,1}(x,t) \\ =&\frac{1}{2}\, \frac{\sqrt{Z}\tau_1 \left( \varepsilon_1 \cosh\left(\frac{1}{2}\sqrt{Z}(-\frac{1}{2}\tau_1 x + \frac{1}{2} Z{\tau_1}^3 t + \gamma)\right) + \varepsilon_2 \sinh\left(\frac{1}{2}\sqrt{Z}(-\frac{1}{2}\tau_1 x + \frac{1}{2} Z{\tau_1}^3 t + \gamma)\right)\right)}{\varepsilon_1 \sinh\left(\frac{1}{2}\sqrt{Z}(-\frac{1}{2}\tau_1 x + \frac{1}{2} Z{\tau_1}^3 t + \gamma)\right) + \varepsilon_2 \cosh\left(\frac{1}{2}\sqrt{Z}(-\frac{1}{2}\tau_1 x + \frac{1}{2} Z{\tau_1}^3 t + \gamma)\right)} \\ &+\tau_0 + \frac{1}{2}\, \frac{\sqrt{Z}\tau_1 \left( \varepsilon_1 \sinh\left(\frac{1}{2}\sqrt{Z}(-\frac{1}{2}\tau_1 x + \frac{1}{2} Z{\tau_1}^3 t + \gamma)\right) + \varepsilon_2 \cosh\left(\frac{1}{2}\sqrt{Z}(-\frac{1}{2}\tau_1 x + \frac{1}{2} Z{\tau_1}^3 t + \gamma)\right)\right)}{\varepsilon_1 \cosh\left(\frac{1}{2}\sqrt{Z}(-\frac{1}{2}\tau_1 x + \frac{1}{2} Z{\tau_1}^3 t + \gamma)\right) + \varepsilon_2 \sinh\left(\frac{1}{2}\sqrt{Z}(-\frac{1}{2}\tau_1 x + \frac{1}{2} Z{\tau_1}^3 t + \gamma)\right)}. \end{aligned} \tag{51}$$

(ii) In the course of $\varepsilon_1 = 0, \varepsilon_2 \neq 0$,

$$\begin{aligned} s_{2,3,2}(x,t) =& \frac{1}{2}\, \frac{\sqrt{Z}\tau_1}{\coth\left(\frac{1}{2}\sqrt{Z}(-\frac{1}{2}\tau_1 x + \frac{1}{2} Z{\tau_1}^3 t + \gamma)\right)} \\ &+ \tau_0 + \frac{1}{2}\tau_1 \sqrt{Z} \coth\left(\frac{1}{2}\sqrt{Z}(-\frac{1}{2}\tau_1 x + \frac{1}{2} Z{\tau_1}^3 t + \gamma)\right). \end{aligned} \tag{52}$$

(iii) In the course of $\varepsilon_1 \neq 0, \varepsilon_2 = 0$,

$$\begin{aligned} s_{2,3,3}(x,t) =& \frac{1}{2}\, \frac{\sqrt{Z}\tau_1}{\tanh\left(\frac{1}{2}\sqrt{Z}(-\frac{1}{2}\tau_1 x + \frac{1}{2} Z{\tau_1}^3 t + \gamma)\right)} \\ &+ \tau_0 + \frac{1}{2}\tau_1 \sqrt{Z} \tanh\left(\frac{1}{2}\sqrt{Z}(-\frac{1}{2}\tau_1 x + \frac{1}{2} Z{\tau_1}^3 t + \gamma)\right). \end{aligned} \tag{53}$$

**Family 2.3.2.** In the course of $Z < 0$,

(i) In the course of $\varepsilon_1 \neq 0, \varepsilon_2 \neq 0$,

$$\begin{aligned} s_{2,3,4}(x,t) =& \frac{1}{2}\, \frac{Z\tau_1 \left( \varepsilon_1 \cos\left(\frac{1}{2}\sqrt{-Z}(-\frac{1}{2}\tau_1 x + \frac{1}{2} Z{\tau_1}^3 t + \gamma)\right) + \varepsilon_2 \sin\left(\frac{1}{2}\sqrt{-Z}(-\frac{1}{2}\tau_1 x + \frac{1}{2} Z{\tau_1}^3 t + \gamma)\right)\right)}{\sqrt{-Z}\left(-\varepsilon_1 \sin\left(\frac{1}{2}\sqrt{-Z}(-\frac{1}{2}\tau_1 x + \frac{1}{2} Z{\tau_1}^3 t + \gamma)\right) + \varepsilon_2 \cos\left(\frac{1}{2}\sqrt{-Z}(-\frac{1}{2}\tau_1 x + \frac{1}{2} Z{\tau_1}^3 t + \gamma)\right)\right)} \\ &+ \tau_0 + \frac{1}{2}\, \frac{\tau_1\sqrt{-Z}\left( -\varepsilon_1 \sin\left(\frac{1}{2}\sqrt{-Z}(-\frac{1}{2}\tau_1 x + \frac{1}{2} Z{\tau_1}^3 t + \gamma)\right) + \varepsilon_2 \cos\left(\frac{1}{2}\sqrt{-Z}(-\frac{1}{2}\tau_1 x + \frac{1}{2} Z{\tau_1}^3 t + \gamma)\right)\right)}{\varepsilon_1 \cos\left(\frac{1}{2}\sqrt{-Z}(-\frac{1}{2}\tau_1 x + \frac{1}{2} Z{\tau_1}^3 t + \gamma)\right) + \varepsilon_2 \sin\left(\frac{1}{2}\sqrt{-Z}(-\frac{1}{2}\tau_1 x + \frac{1}{2} Z{\tau_1}^3 t + \gamma)\right)}. \end{aligned} \tag{54}$$

(ii) In the course of $\varepsilon_1 = 0, \varepsilon_2 \neq 0$,

$$s_{2,3,5}(x,t) = \frac{1}{2}\frac{Z\tau_1}{\sqrt{-Z}\cot\left(\frac{1}{2}\sqrt{-Z}(-\frac{1}{2}\tau_1 x + \frac{1}{2}Z{\tau_1}^3 t + \gamma)\right)} + \tau_0 + \frac{1}{2}\tau_1\sqrt{-Z}\cot\left(\frac{1}{2}\sqrt{-Z}(-\frac{1}{2}\tau_1 x + \frac{1}{2}Z{\tau_1}^3 t + \gamma)\right). \tag{55}$$

(iii) In the course of $\varepsilon_1 \neq 0, \varepsilon_2 = 0$,

$$s_{2,3,6}(x,t) = -\frac{1}{2}\frac{Z\tau_1}{\sqrt{-Z}\tan\left(\frac{1}{2}\sqrt{-Z}(-\frac{1}{2}\tau_1 x + \frac{1}{2}Z{\tau_1}^3 t + \gamma)\right)} + \tau_0 - \frac{1}{2}\tau_1\sqrt{-Z}\tan\left(\frac{1}{2}\sqrt{-Z}(-\frac{1}{2}\tau_1 x + \frac{1}{2}Z{\tau_1}^3 t + \gamma)\right). \tag{56}$$

**Family 2.3.3.** In the course of $Z = 0$,

(i) In the course of $\varepsilon_1 \neq 0, \varepsilon_2 \neq 0$,

$$s_{2,3,7}(x,t) = \frac{1}{4}Z\tau_1\left(\frac{1}{2}\nu + \frac{\varepsilon_2}{\varepsilon_1 + \varepsilon_2(-\frac{1}{2}\tau_1 x + \frac{1}{2}Z{\tau_1}^3 t + \gamma)}\right)^{-1} + \tau_0 + \tau_1\left(\frac{1}{2}\nu + \frac{\varepsilon_2}{\varepsilon_1 + \varepsilon_2(-\frac{1}{2}\tau_1 x + \frac{1}{2}Z{\tau_1}^3 t + \gamma)}\right). \tag{57}$$

(ii) In the course of $\varepsilon_1 = 0, \varepsilon_2 \neq 0$,

$$s_{2,3,8}(x,t) = \frac{1}{4}Z\tau_1(-\frac{1}{2}\tau_1 x + \frac{1}{2}Z{\tau_1}^3 t + \gamma) + \tau_0 + \frac{\tau_1}{(-\frac{1}{2}\tau_1 x + \frac{1}{2}Z{\tau_1}^3 t + \gamma)}. \tag{58}$$

## 4. Graphical discussion

In this research paper, we display the frameworks of the several wave types contained in the model. Two refined versions of the $(\frac{G'}{G})$-expansion approach were used to extract and clearly demonstrate wave patterns for solitons in 2D, contour and 3D forms. Gaining a knowledge of these notions is necessary to comprehend the behavior of linked physical events. It is anticipated that the found soliton solutions would greatly advance our understanding about the model's underlying behavior. Moreover, it is illustrated visually that the solitons display kink-type behaviors such as solitary kink, anti-kink, dark-bright kink, periodic kink, multiple kink and dark kink in the K-XE scenario. In the realm of K-XE, a soliton is an autonomous wave that moves through the medium without altering its form or speed. The stability and self-organizing ability of these waves is widely known, even after they collide and interact with other comparable solitons. A kink type soliton is a localized wave that exhibits discontinuity or phase change. It is distinguished by abrupt changes in phase or state, resembling a step or kink-like patterns in the profile.

The K-XE is related to curve differential geometry and is essential to comprehending solitons' behavior in nonlinear systems. The given equation captures the geometric characteristics and equivalency classifications of curves in a range of physical models, resulting in a variety of kink solitons in the K-XE scenario, including solitary, dark, dark-bright, anti-, multiple, and periodic kinks. Every kind of soliton embodies a distinct geometrical and physical characteristic that provides information about nonlinear wave processes in a variety of scientific domains. With its foundations in differential geometry, the K-XE offers a flexible framework for comprehending these solitonic tendencies. A solitary kink soliton is an example of a confined, smoothed waveform that alternates between two different asymptotic phases. It features an individual transitioning point and an established framework. A kink soliton of this kind results from the interaction of dispersion and nonlinear processes. This model's curve shape makes it possible to allow such a shift to happen seamlessly. The term "solitary kink" in differential geometry refers to a shift in a surface's or curve's curvature when the soliton travels across the geometry with no dissipating. In studying the phenomenon of transitions in phase, which are the shifts between two distinct states of a system devoid of oscillatory activity, this soliton is important. It frequently simulates fluid interfaces or magnetic domain barriers. A dark kink soliton is defined by a zone of dropped wave magnitude (a trough) which splits two steady surroundings states. The variation of the system's curvature in the K-XE causes dark kinks, and the soliton is a confined decrease in wave amplitude. Geometrically stated, the dark kink is the result of a wave dipping into a low-energy state, smoothing or reducing the shape of the curve. In optical structures, Bose-Einstein condensates, and fluid mechanics, dark kinks are important because they symbolize phase shifts or transition in areas with little density. A combined soliton with bright patches around a dark zone (the depletion in wave intensity) (the elevation in waveform amplitude) is called a dark-bright kink. This soliton frequently entails the interplay of two distinct wave modes. The K-XE's shape permits both dark and light constituents to coexist inside of an individual soliton framework, balancing the differential curvature of several interacting curves. These solitons play a crucial role in multi-component systems where diverse modes interplay to form confined nanostructures with distinct potential states, such are linked optic fibers or plasma dynamics. Dark-bright kinks, for example, simulate the connection between varying light concentrations in optical networks, where a particular mode is in a low-energy phase (dark) while the other one is in a high-energy phase (bright). The reverse of a solitary kink is called an anti-kink soliton. It denotes a change in direction when the wave, following an initial disturbance, returns to its starting condition. The solution when the underlying geometric curve's curvature flips or flips orientation is known as the anti-kink. It demonstrates the structure's symmetry and balances the solitary kink. The anti-kink in curve geometry is an inversion in a curve's pitch or flexing, resulting in a reverse transition. Multiple kinks that occur sequentially, signifying various state transitions, are represented by multiple kink soliton structures. The ability of the K-XE framework to characterize the interactions between various curvature transitions implies the presence of many kink solutions. A sequence of abrupt changes in a curve's or surface's curvature when the system switches between distinct geometric configurations is represented by many kinks in differential geometry. Such solitons represent numerous intersections or transitioning between various areas, and are used to describe complicated, multistate entities such as multilayer mediums or multi-domain magnetized systems. Finally, a periodic kink soliton is characterized by an oscillating, repeating pattern in which the kink recurs throughout either space or time. Because of the K-XE's intrinsic symmetry and boundary requirements, which let kink flips to reoccur, the kink soliton exhibits periodicity. From a geometric perspective, this denotes a recurring periodic modulation in a surface's or curve's curvature. Systems have periodic potentials, such as crystals or waveguides that have periodic kinks because of the geometry of the lattice or exogenous periodic forces that cause solitons to travel in a predictable, repeating manner.

**Remark 1.** Figure 1 is presented for $s_{1,1,3}(x,t)$ in Eq (17) which shows kink soliton profile.

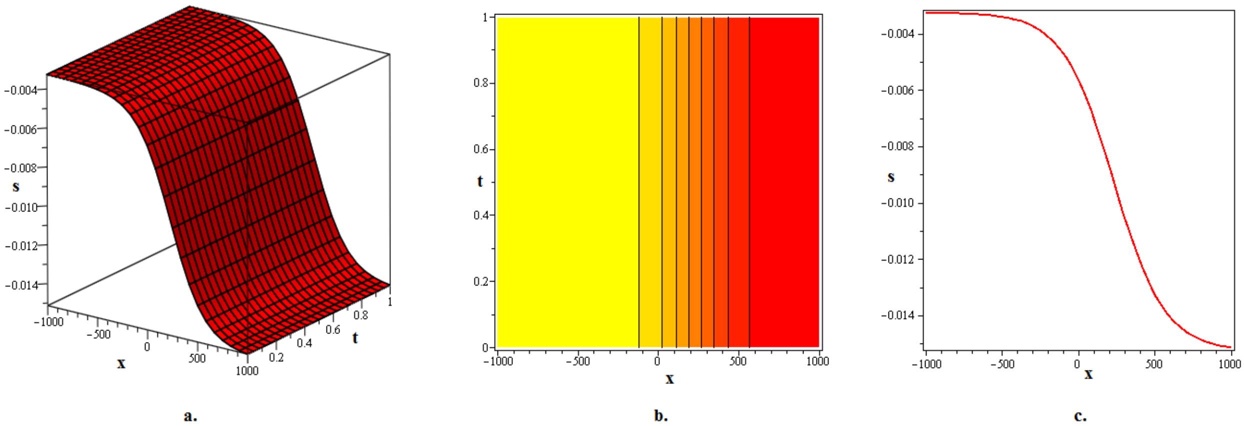


**Figure 1.** These 3-D, contour and 2-D (when $t = 0$) plots of the kink soliton solution $s_{1,1,3}$, expressed in Eq (17), are depicted for $\nu = 10; \omega = 16, \gamma = 0.0001, k = 0.001, \tau_0 = 0.00075$.

**Remark 2.** Figure 2 is presented for $s_{1,1,5}(x,t)$ in Eq (19) which shows the dark-bright kink soliton profile.

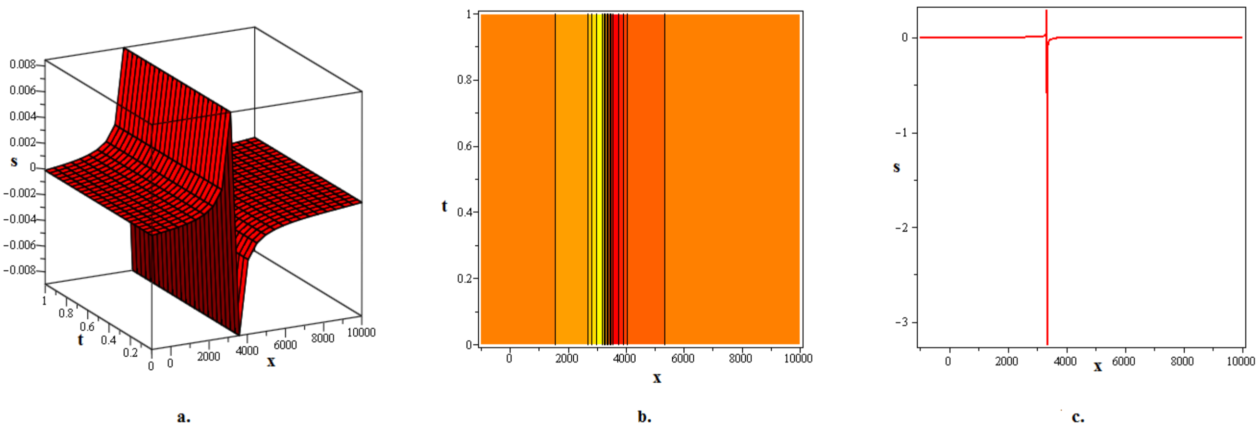


**Figure 2.** These 3-D, contour and 2-D (when $t = 1$) plots of the kink soliton solution $s_{1,1,5}$, expressed in Eq (19), are depicted for $\nu = 2, \omega = 3, \gamma = 0.005, k = 0.0002, \tau_0 = 0.0001$.

**Remark 3.** Figure 3 is presented for $s_{1,2,3}(x,t)$ in Eq (25) which shows the kink soliton profile.

**Remark 4.** Figure 4 is presented for $s_{1,2,6}(x,t)$ in Eq (28) which shows the multiple periodic-kink soliton profile.

**Remark 5.** Figure 5 is presented for $s_{2,1,2}(x,t)$ in Eq (36) which shows the dark-bright kink soliton profile.

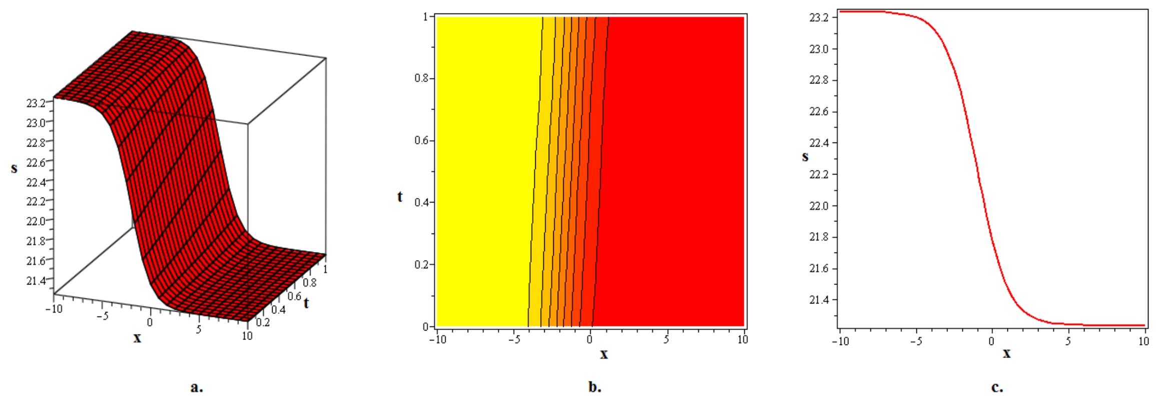


**Figure 3.** These 3-D, contour and 2-D (when $t = 1$) plots of the kink soliton solution $s_{1,2,3}$, expressed in Eq (25), are depicted for $\nu = \sqrt(5), \omega = 1, \gamma = 2, k = 1, \tau_0 = 20$.

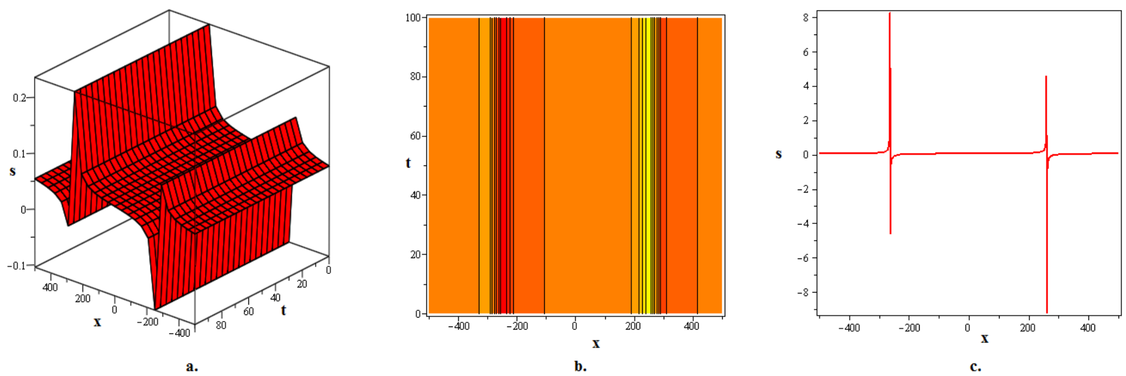


**Figure 4.** These 3-D, contour and 2-D (when $t = 10$) plots of the kink soliton solution $s_{1,2,6}$, expressed in Eq (28), are depicted for $\nu = 2, \omega = 5, \gamma = 0.002, k = 0.003E, \tau_0 = 0.005$.

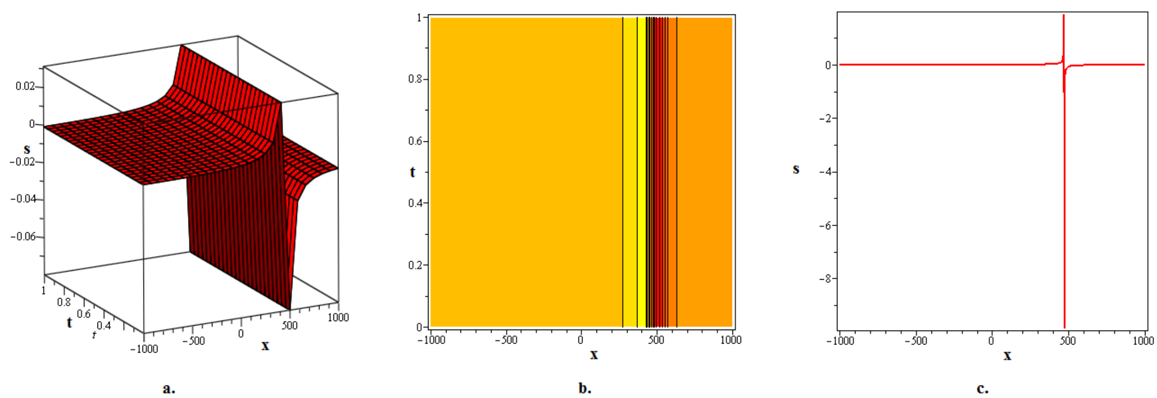


**Figure 5.** These 3-D, contour and 2-D (when $t = 0$) plots of the kink soliton solution $s_{2,1,2}$, expressed in Eq (36), are depicted for $\nu = 5, \omega = 4, k = 0.001, \gamma = 0.00001, r = 0.045, \tau_0 = 0.0010$.

**Remark 6.** Figure 6 is presented for $s_{2,1,3}(x,t)$ in Eq (37) which shows the anti-kink soliton profile.

**Remark 7.** Figure 7 is presented for $s_{2,2,1}(x,t)$ in Eq (43) which shows the kink soliton profile.

**Remark 8.** Figure 8 is presented for $s_{2,2,4}(x,t)$ in Eq (46) which shows the kink soliton profile.

**Remark 9.** Figure 9 is presented for $s_{2,3,3}(x,t)$ in Eq (53) which shows the kink soliton profile.

**Remark 10.** Figure 10 is presented for $s_{2,3,5}(x,t)$ in Eq (55) which shows the dark-kink soliton profile.

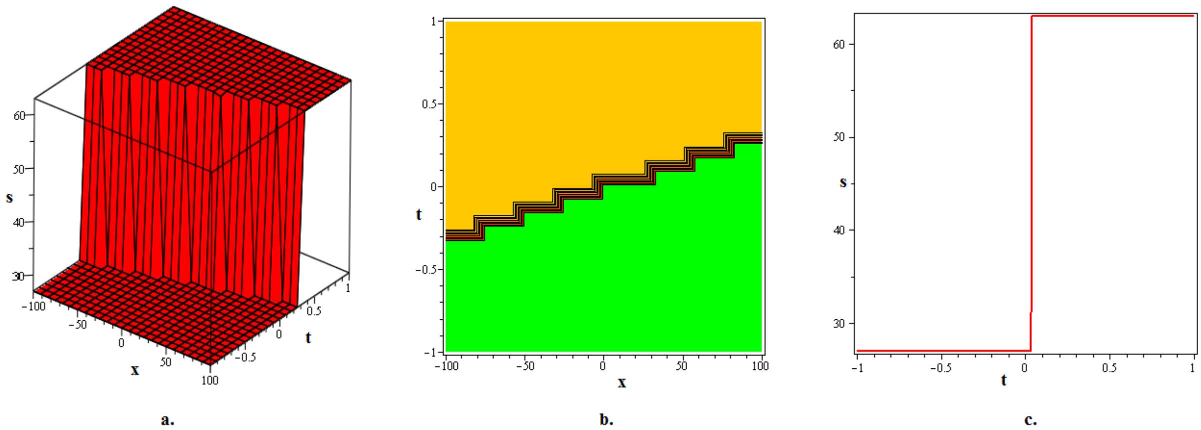


**Figure 6.** These 3-D, contour and 2-D (when $x = 10$) plots of the kink soliton solution $s_{2,1,3}$, expressed in Eq (37), are depicted for $\nu = 10, \omega = 16, k = 3, \gamma = 5, r = 10, \tau_0 = 15$.

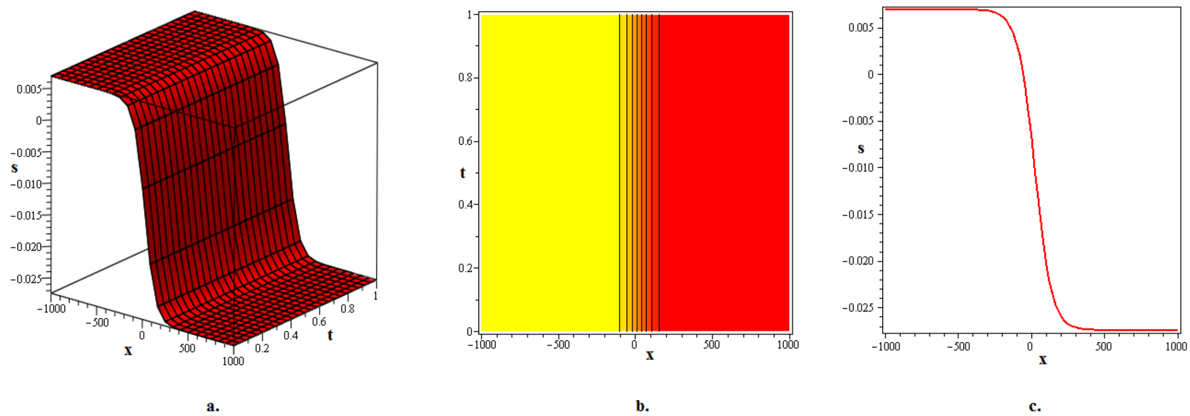


**Figure 7.** These 3-D, contour and 2-D (when $t = 0.1$) plots of the kink soliton solution $s_{2,2,1}$, expressed in Eq (43), are depicted for $\nu = 5, \omega = 1, \gamma = 0.0004, r = 1, \tau_1 = 0.0075, \tau_0 = 0.001, \varepsilon_1 = 0.005, \varepsilon_2 = 0.0010$.

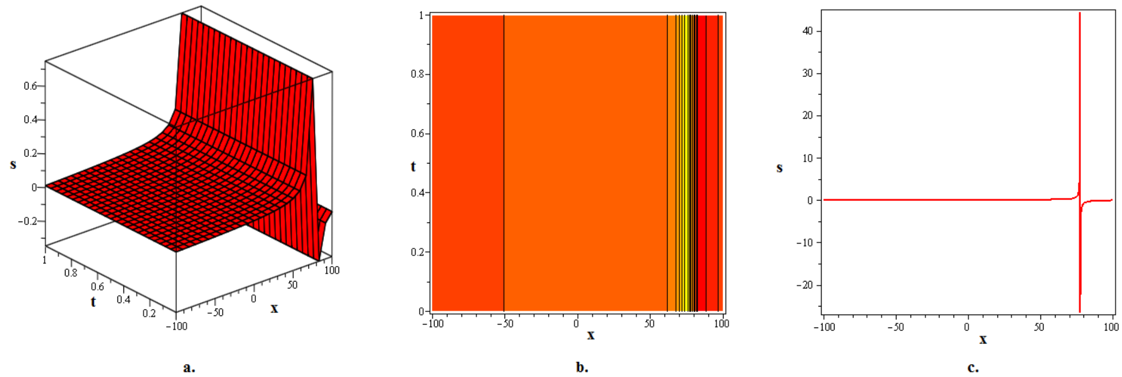


**Figure 8.** These 3-D, contour and 2-D (when $t = 0$) plots of the kink soliton solution $s_{2,2,4}$, expressed in Eq (46), are depicted for $\nu = 1, \omega = 3, \gamma = 0.0005, r = 1, \tau_1 = 0.01, \tau_0 = 0.005, \varepsilon_1 = 3, \varepsilon_2 = 4$.

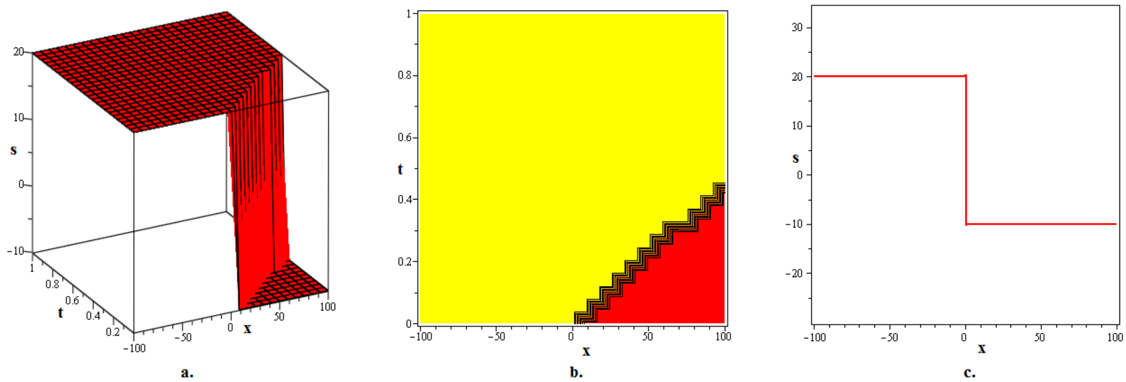


**Figure 9.** These 3-D, contour and 2-D (when $t = 0$) plots of the kink soliton solution $s_{2,3,3}$, expressed in Eq (53), are depicted for $\nu = 13, \omega = 36, \gamma = 1, r = 2, \tau_1 = 3, \tau_0 = 5, \varepsilon_1 = 10, \varepsilon_2 = 20$.

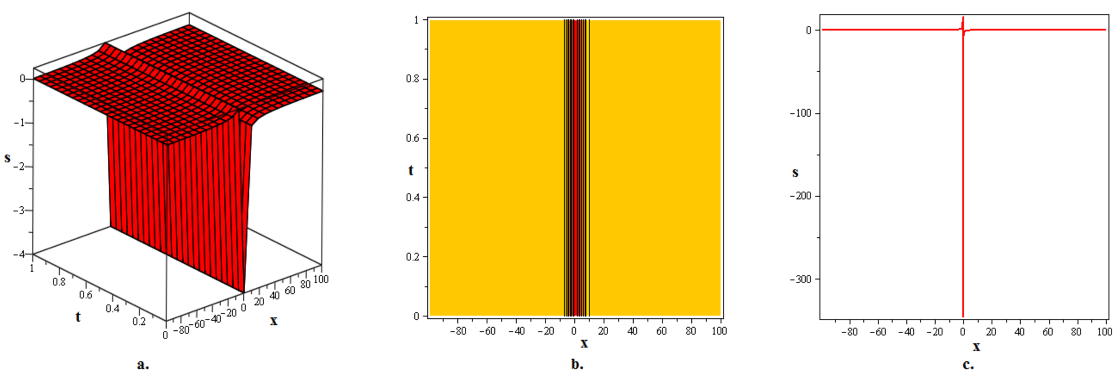


**Figure 10.** These 3-D, contour and 2-D (when $t = 0.5$) plots of the kink soliton solution $s_{2,3,5}$, expressed in Eq (55), are depicted for $\nu = 0, \omega = 4, \gamma = 0, \tau_1 = 0.00010, \tau_0 = 0.00005$.

## 5. Conclusions

In order to address the crucial integrable model that explains the differential geometry of curves and equivalence aspects dubbed K-XE, two updated variations of the $(\frac{G'}{G})$-expansion approach were employed in this work namely the simple $(\frac{G'}{G})$-expansion method and the generalized $(r+\frac{G'}{G})$-expansion method. Using the recommended methods, the single NODEs that the model produced are solved in sequence. Next, we transformed this solution into a system of nonlinear algebraic equations, leading to new families of soliton solutions that are essential to understanding the model from a physical perspective. Several 3-D, 2-D, and contour graphs demonstrated that the acquired solitons likely take the structures of kink solitons prominently. The work highlights the potential consequences for several practical applications in the associated domains and demonstrates how the proposed methodologies may be utilized to generate families of soliton solutions for nonlinear models. Additionally, compared to the simple $(\frac{G'}{G})$-expansion method, the generalized $(r + \frac{G'}{G})$-expansion method can be considered more efficient because it yields a large number of fresh plethora of soliton solutions that contribute to our comprehension and help to make sense of the complex dynamics of the model. Although the $(\frac{G'}{G})$-expansion method has greatly advanced our knowledge of soliton dynamics and how they relate to the models we study, it is crucial to recognize the method's shortcomings, especially now the proposed method fails in cases where the highest derivative term and nonlinear term cannot be balanced. Despite this drawback, the current study shows that the approach used in this work is very robust, portable, and effective for nonlinear issues across a range of natural science fields. Moreover, the future goal of this investigation is to delve into the stability analysis of solitons and the incorporation and impact of the fractional derivatives on solitons in the realm of the aimed model.

## Author contributions

Conceptualization, R.Q; Data curation, N.M.A.A.; Formal analysis, H.Z; Resources, A.A.F; Investigation, R.Q; Project administration, N.M.A.A; Validation, H.Z.; Software, A.A.F; Validation, R.Q; Visualization, N.M.A.A.; Validation, H.Z.; Visualization, N.M.A.A.; Resources, H.Z.; Project administration, A.A.F.; Writingreview & editing, H.Z.; Funding, R.Q. All authors have read and agreed to the published version of the manuscript.

## Acknowledgments

The authors gratefully acknowledge the funding of the Deanship of Graduate Studies and Scientific Research, Jazan University, Saudi Arabia, through Project Number: GSSRD-24.

## Conflict of interest

The authors declare that they have no conflicts of interest.

## References

1. Y. Swapna, Applications of partial differential equations in fluid physics, *Commun. Appl. Nonlinear Anal.*, **31** (2024), 207–220. https://doi.org/10.52783/cana.v31.396

2. A. Cheviakov, P. Zhao, *Analytical properties of nonlinear partial differential equations: with applications to shallow water models*, Vol. 10, Springer Cham, 2024. https://doi.org/10.1007/978-3-031-53074-6
3. A. H. Ganie, L. H. Sadek, M. M. Tharwat, M. A. Iqbal, M. M. Miah, M. M. Rasid, et al., New investigation of the analytical behaviors for some nonlinear PDEs in mathematical physics and modern engineering, *Partial Differ. Equations Appl. Math.*, **9** (2024), 100608. https://doi.org/10.1016/j.padiff.2023.100608
4. J. L. Kazdan, *Applications of partial differential equations to problems in geometry*, Graduate Texts in Mathematics, 1983.
5. H. Khan, R. Shah, J. F. Gómez-Aguilar, Shoaib, D. Baleanu, P. Kumam, Travelling waves solution for fractional-order biological population model, *Math. Model. Nat. Phenom.*, **16** (2021), 32. https://doi.org/10.1051/mmnp/2021016
6. A. P. Bassom, P. A. Clarkson, A. C. Hicks, On the application of solutions of the fourth Painlev equation to various physically motivated nonlinear partial differential equations, *Adv. Differ. Equations*, **1** (1996), 175–198. https://doi.org/10.57262/ade/1366896236
7. P. Albayrak, M. Ozisik, M. Bayram, A. Secer, S. E. Das, A. Biswas, et al., Pure-cubic optical solitons and stability analysis with Kerr law nonlinearity, *Contemp. Math.*, **4** (2023), 530-548. https://doi.org/10.37256/cm.4320233308
8. S. Altun, M. Ozisik, A. Secer, M. Bayram, Optical solitons for Biswas-Milovic equation using the new Kudryashov's scheme, *Optik*, **270** (2022), 170045. https://doi.org/10.1016/j.ijleo.2022.170045
9. E. M. Zayed, A. H. Arnous, A. Secer, M. Ozisik, M. Bayram, N. A. Shah, et al., Highly dispersive optical solitons in fiber Bragg gratings for stochastic Lakshmanan-Porsezian-Daniel equation with spatio-temporal dispersion and multiplicative white noise, *Results Phys.*, **55** (2023), 107177. https://doi.org/10.1016/j.rinp.2023.107177
10. M. S. Islam, K. Khan, M. A. Akbar, The generalized Kudrysov method to solve some coupled nonlinear evolution equations, *Asian J. Math. Comput. Res.*, **3** (2015), 104–121.
11. R. Ali, E. Tag-eldin, A comparative analysis of generalized and extended $(\frac{G'}{G})$-Expansion methods for travelling wave solutions of fractional Maccari's system with complex structure, *Alexandria Eng. J.*, **79** (2023), 508–530. https://doi.org/10.1016/j.aej.2023.08.007
12. M. Cinar, A. Secer, M. Ozisik, M. Bayram, Derivation of optical solitons of dimensionless Fokas-Lenells equation with perturbation term using Sardar sub-equation method, *Opt. Quant. Electron.*, **54** (2022), 402. https://doi.org/10.1007/s11082-022-03819-0
13. M. Dehghan, J. Manafian Heris, A. Saadatmandi, Application of the Exp-function method for solving a partial differential equation arising in biology and population genetics, *Int. J. Numer. Methods Heat Fluid Flow*, **21** (2011), 736–753. https://doi.org/10.1108/09615531111148482
14. A. Bekir, E. Aksoy, A. C. Cevikel, Exact solutions of nonlinear time fractional partial differential equations by sub-equation method, *Math. Methods Appl. Sci.*, **38** (2015), 2779–2784. https://doi.org/10.1002/mma.3260

15. M. Kamrujjaman, A. Ahmed, J. Alam, Travelling waves: interplay of low to high Reynolds number and Tan-Cot function method to solve Burgers equations, *J. Appl. Math. Phys.*, **7** (2019), 861. https://doi.org/10.4236/jamp.2019.74058

16. S. Noor, A. S. Alshehry, A. Khan, I. Khan, Analysis of soliton phenomena in (2 + 1)-dimensional Nizhnik-Novikov-Veselov model via a modified analytical technique, *AIMS Math.*, **8** (2023), 28120–28142. https://doi.org/10.3934/math.20231439

17. R. Ali, S. Barak, A. Altalbe, Analytical study of soliton dynamics in the realm of fractional extended shallow water wave equations, *Phys. Scr.*, **99** (2024), 065235. https://doi.org/10.1088/1402-4896/ad4784

18. M. M. Tariq, M. B. Riaz, M. Aziz-ur-Rehman, Investigation of space-time dynamics of Akbota equation using Sardar sub-equation and Khater methods: unveiling bifurcation and chaotic structure, *Int. J. Theor. Phys.*, **63** (2024), 210. https://doi.org/10.1007/s10773-024-05733-5

19. X. Yang, Z. Wang, Z. Zhang, Decay mode ripple waves within the (3 + 1)-dimensional Kadomtsev-Petviashvili equation, *Math. Methods Appl. Sci.*, **47** (2024), 10444-10461. https://doi.org/10.1002/mma.10132

20. A. H. Ganie, M. M. AlBaidani, A. M. Wazwaz, W. X. Ma, U. Shamima, M. S. Ullah, Soliton dynamics and chaotic analysis of the Biswas-Arshed model, *Opt. Quant. Electron.*, **56** (2024), 1379. https://doi.org/10.1007/s11082-024-07291-w

21. M. Wang, X. Li, J. Zhang, The $(\frac{G'}{G})$-expansion method and travelling wave solutions of nonlinear evolution equations in mathematical physics, *Phys. Lett. A*, **372** (2008), 417–423. https://doi.org/10.1016/j.physleta.2007.07.051

22. E. H. M. Zahran, M. M. A. Khater, Modified extended tanh-function method and its applications to the Bogoyavlenskii equation, *Appl. Math. Model.*, **40** (2016), 1769–1775. https://doi.org/10.1016/j.apm.2015.08.018

23. Z. Myrzakulova, S. Manukure, R. Myrzakulov, G. Nugmanova, Integrability, geometry and wave solutions of some Kairat equations, *arXiv*, 2023. https://doi.org/10.48550/arXiv.2307.00027

24. M. Awadalla, A. Zafar, A. Taishiyeva, M. Raheel, R. Myrzakulov, A. Bekir, The analytical solutions to the M-fractional Kairat-II and Kairat-X equations, *Front. Phys.*, **11** (2023), 1335423.

25. S. Roy, S. Raut, R. Myrzakulov, Z. Umurzakhova, A Kairat-X equation and its integrability: shocks, lump-kink and kinky-breather, *CC BY 4.0*, 2023. https://doi.org/10.13140/RG.2.2.23245.20963

26. S. Ghazanfar, N. Ahmed, M. S. Iqbal, A. Akgül, M. Bayram, M. De la Sen, Imaging ultrasound propagation using the Westervelt equation by the generalized Kudryashov and modified Kudryashov methods, *Appl. Sci.*, **12** (2022), 11813. https://doi.org/10.3390/app122211813

27. G. H. Tipu, W. A. Faridi, Z. Myrzakulova, R. Myrzakulov, S. A. AlQahtani, N. F. AlQahtani, et al., On optical soliton wave solutions of non-linear Kairat-X equation via new extended direct algebraic method, *Opt. Quant. Electron.*, **56** (2024), 655. https://doi.org/10.1007/s11082-024-06369-9

28. M. Iqbal, D. Lu, A. R. Seadawy, F. A. H. Alomari, Z. Umurzakhova, R. Myrzakulov, Constructing the soliton wave structure to the nonlinear fractional Kairat-X dynamical equation under computational approach, *Mod. Phys. Lett. B*, 2024, 2450396. https://doi.org/10.1142/S0217984924503962

29. S. Sirisubtawee, S. Koonprasert, S. Sungnul, New exact solutions of the conformable space-time Sharma-Tasso-Olver equation using two reliable methods, *Symmetry*, **12** (2020), 644. https://doi.org/10.3390/sym12040644